13th World Conference on Earthquake Engineering
Vancouver, B.C., Canada
August 1-6, 2004
Paper No. 102

SEISMIC UPGRADE OF SLAB-COLUMN CONNECTIONS USING CARBON FIBER REINFORCEMENT

Andrew STARK[1], Baris BINICI[2], and Oguzhan BAYRAK[3]

INTRODUCTION

Flat plate structures are commonly used in moderate and low seismic zones as lateral force resisting systems whereas they are coupled with shear walls or moment resisting frames in high seismic zones. The ductility of these systems is generally limited by the deformation capacity of the slab-column connections. Punching shear failure is the governing failure mode in the presence of pronounced gravity and lateral load combinations. The ductility of the slab-column connections can be enhanced with the use of shear reinforcement for new construction [1, 2] and the risk of punching shear failure can be highly reduced when the connection is designed and detailed properly. The research results presented here provides an alternative method for upgrading existing flat plate building connections that were designed to carry gravity loads and that are subjected to lateral deformation reversals.

The results of an experimental program on seismic upgrade of slab-column connections are presented in this paper. All slab-column connections were upgraded by externally installed CFRP stirrups in two different patterns. Specimens were tested under constant gravity shear and lateral displacements were applied in a reversed cyclic manner. Punching shear failure occurred for the control specimens at a lateral drift-ratio of about 2.3%. Upgraded specimens had significant flexural yielding and sustained deformations up to a drift ratio of about 8% without significant losses of strength. Punching failure was not observed in the upgraded specimens.

BACKGROUND

There have been a number of studies to understand lateral load behavior of flat plate systems under constant gravity shear. Experiments were conducted on isolated interior and exterior slab-column connections [1, 3-9] and on flat plate sub-assemblages [10-12]. The results of the experiments provided information on the lateral stiffness, strength, ductility, and insight on the cyclic behavior of the slab-column connections of reinforced concrete flat plate systems. It was found that gravity shear is the most important factor affecting the ductility of the connections under cyclic load reversals. Detailed reviews of

---

[1] Graduate Research Assistant, The University of Texas at Austin, Austin, TX.
[2] Faculty Member, Department of Civil Engineering, Middle East Technical University, Ankara, Turkey.
[3] Assistant Professor of Civil Engineering, Ferguson Structural Engineering Laboratory, The University of Texas at Austin, Austin, TX.

these experimental studies can be found elsewhere [8, 13, 14]. These studies showed that when the gravity shear ratio (ratio of gravity shear to concentric punching shear capacity) was about 0.4, the available displacement ductility of the slab-column connection was about 2 [15]. Considering this, ACI 318-02 recommends limiting the gravity shear ratio to 0.4 for slab-column connections of flat plates at high seismic zones.

Some of the slab-column connections of older flat plate structures that were built in 1960s and 1970s do not comply with requirements of shear reinforcement. In addition, increased levels of gravity loads compared to design loads may necessitate upgrade of slab-column connections to increase punching shear resistance. There is a limited amount of research available on strengthening of slab-column connections. Results of laterally loaded flat plates strengthened using steel and concrete drop panels to increase punching shear strength were presented by Martinez et. al. [16]. Repair of damaged slab-column connections was performed by Farhey et. al. [17] by using externally bolted steel plates and replacing the damaged reinforcement and concrete. Ebead and Marzouk [18] used steel bolts as shear reinforcement together with steel plates at the top and bottom surface of slabs. El-Salakawy et. al. [19] tested full-scale reinforced concrete slab-column edge connections strengthened using externally installed bolts in holes drilled through the slab thickness. The strengthened flat plate specimens were subjected to monotonic and cyclic unbalanced moments [16-19]. The use of externally built column capitals, steel plates and bolts resulted in higher punching shear strength, stiffness and deformation capacity of the slab-column connections in some cases. However, these applications resulted in unfavorable slab thickness increases around the slab column connections. Furthermore, difficulties experienced in site applications of alternatives such as externally built steel drop panels made some of these applications less attractive [20].

RESEARCH SIGNIFICANCE

This study investigates the application of a seismic upgrade method to increase punching shear and deformation capacity of slab-column connections using CFRPs. CFRP strips bonded to concrete in the vertical direction using epoxy are utilized as shear reinforcement around the connection area. This technique can be adopted as a strengthening scheme in flat plate building systems that are vulnerable to punching shear failures. The research results presented here provides an alternative method for upgrading existing flat plate building connections that were designed to carry gravity loads and that are subjected to lateral deformation reversals.

EXPERIMENTAL PROGRAM

Test specimens in the study were modeled from a typical interior connection of a four-story prototype structure [21]. The prototype structure of this study was a flat-plate concrete building, designed for office occupancy in a moderate seismic zone. Gravity moments were calculated using the ACI 318-02 [22] Direct Design Method and seismic lateral loads were determined using IBC 2000. An interior flat-plate slab-column assemblage within the prototype structure was constructed at approximately half scale for the experimental phase of the study. Slab dimensions for all the specimens were 2800 mm x 2800 mm x 115 mm.

Test specimens C-02, A4-S and B4-S were detailed according to section 21.12.6 of ACI 318-02, using the nominal reinforcement ratios specified from the prototype structure design. Figure 1 shows a detail of the bottom and top mats of flexural reinforcement. Test specimen C-63 was detailed according to ACI 318-63 where two bars passing within the column core were discontinuous. Specimens C-02 and C-63 were not upgraded whereas specimens A4-S and B4-S were strengthened using CFRPs acting as shear reinforcement [21].

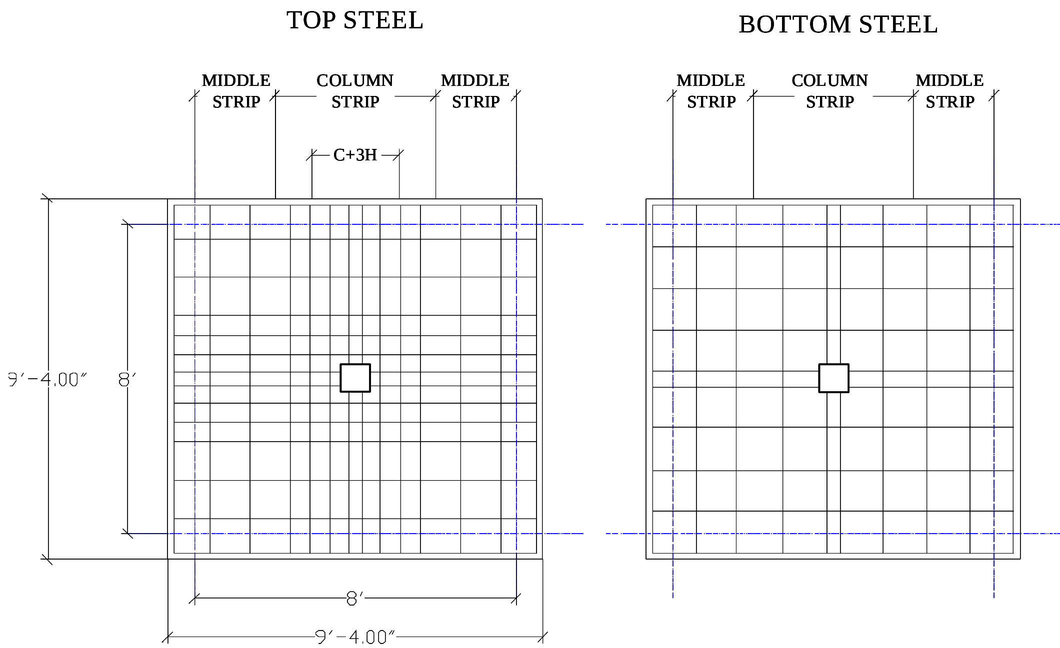

Figure 1 Details of steel reinforcement

In order to upgrade the connection regions of the specimens, CFRP stirrups were added in perimeters around the column in two alternate configurations, denoted A4-S and B4-S. Figure 2 shows a plan view sketch of the two upgrade configurations. The basis for the upgrade configuration was derived from concentric flat-plate punching tests upgraded with CFRP stirrups performed by Binici [23]. In those tests, CFRP stirrups were installed radially in multiple perimeters with different amounts and configurations around the slab-column interface. A similar strategy was used in this study with the two promising CFRP stirrup configurations that correspond to two strengthening patterns as obtained from Binici [23]. For upgrade specimens A4-S and B4-S, a total of four CFRP stirrup perimeters were calculated to be sufficient to change the failure mode from shear to flexure dominated based on strength calculations as recommended by ACI 318-02.

After the column sections (top and bottom) were fixed to the slab with the use of eight bolts, CFRP stirrups were installed to strengthen the connection regions of specimens A4-S and B4-S. Pressurized air was used to clean out debris accrued from slab movement and the column being fixed. Fiber strips were then cut to appropriate length and width from a stock roll of carbon fiber fabric. 19 mm wide CFRP strips were used as stirrups for the upgraded specimen, which required two layers of CFRP per hole in the slab. Holes were created prior to casting using PVC pipes in specified patterns around the possible slab-column connection area. Two part epoxy was proportioned and mixed. After impregnating the CFRPs with epoxy, CFRP strips were weaved from one hole to the next to form closed loop stirrups. To develop the strength of the CFRP strips, 152 mm of CFRP material were overlapped when constructing the stirrups. The CFRP stirrups were allowed to cure at least three days prior to testing.

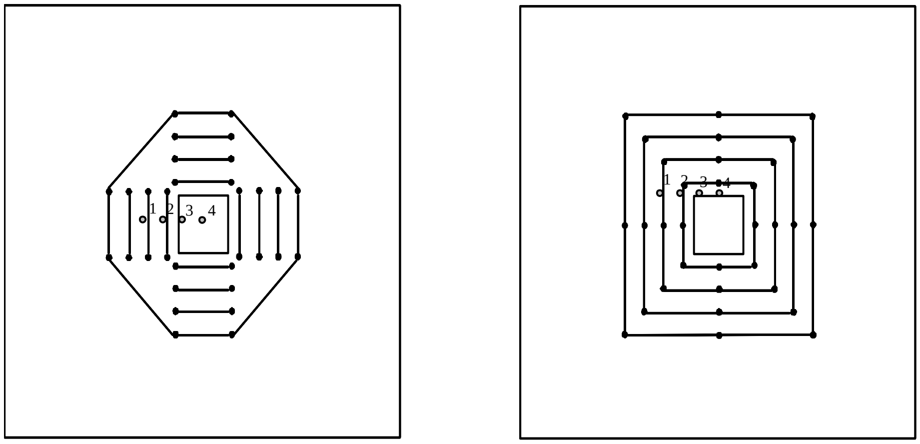

∘ CFRP strain gauge locations for Table 1.

a) Specimen A4-S b)Specimen B4-S

Figure 2 Connection upgrade configurations (plan view)

A schematic of the test setup is shown in Figure 3. Gravity load was applied to each specimen using a hydraulic jack and a load maintainer. Lateral displacements were applied using a horizontal hydraulic actuator at the top of each specimen's column and resisted by a horizontal strut attached.

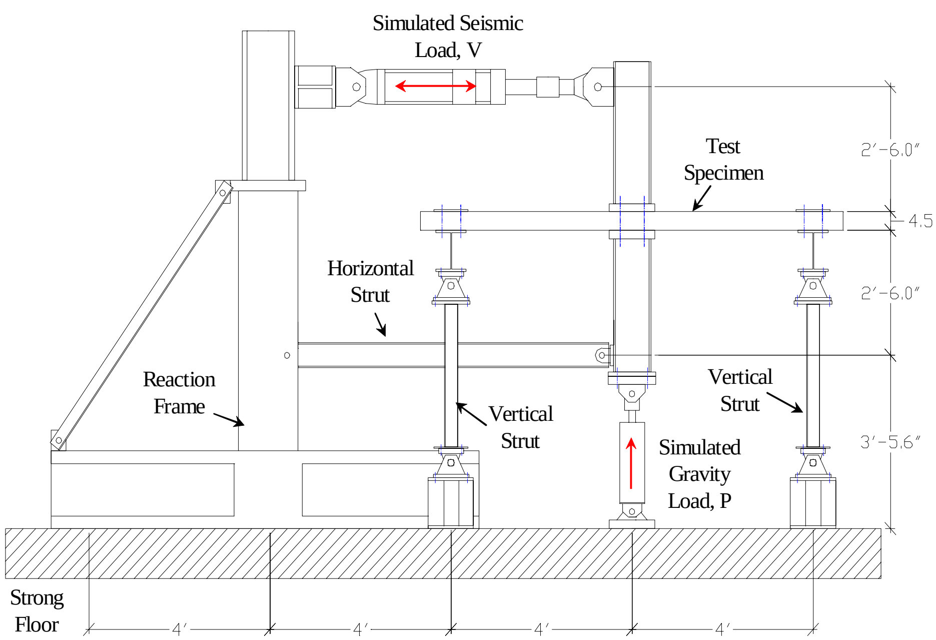

Figure 3 Test setup

The lateral displacement protocol (Figure 4) was a modified version of ACI ITG/T1.1-99, Acceptance Criteria for Moment Frames Based on Structural Testing [24]. Three fully reversed displacement cycles were applied to each specimen from drift ratios of 0.25% to 6%. Two fully reversed cycles were applied to each test specimen upon reaching a drift ratio of 6%.

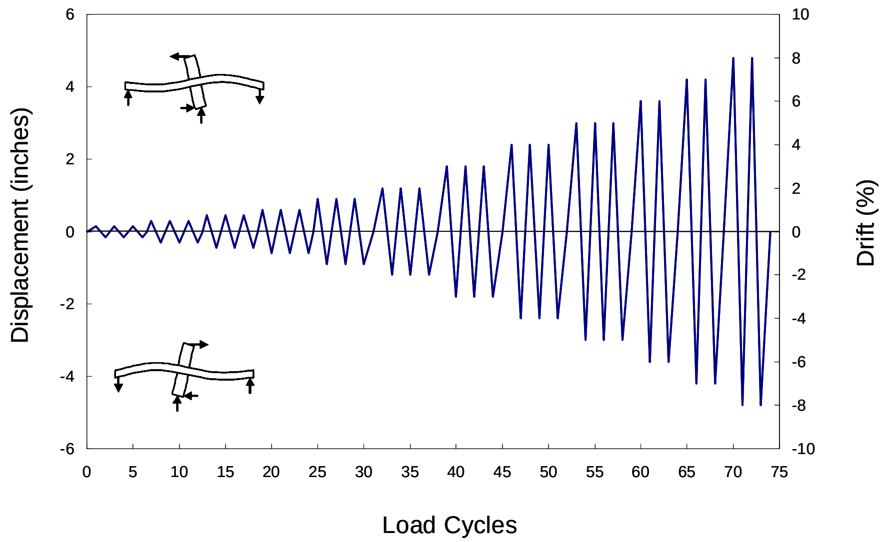

Figure 4 Lateral displacement protocol

Prior to testing, each test specimen was extensively instrumented to measure lateral and gravity loads (load cells), column and slab displacements (linear potentiometers), connection and column rotations (inclinometers), CFRP strains. Strain gauges were bonded to the CFRP stirrups, in the vertical holes through the slab, prior to filling the holes with epoxy. Complete details of instrumentation, testing and results can be found elsewhere [21].

TEST RESULTS

Lateral load versus drift ratio and for test specimens C-02, C-63, A4-S and B4-S are shown in Figures 5 to 8. Lateral inter-story drift ratio was defined as the horizontal displacement of the top column relative to the bottom column, divided by the height of the column.

Control specimens C-02 and C-63 exhibited punching shear failures that resulted in a significant drop in lateral load. At a drift ratio of about 2%, cracks began to open and considerable pinching occurred in the lateral load-deformation plots (Figures 7 and 8). Concrete began to spall around each specimen's column base plate, on the bottom slab face, prior to punching shear failure. Punching initiated on the north side of the column of specimen C-63 at a drift ratio of 2.26% and punched on the south side at an applied drift ratio of 1.38%. At this point, the punching cone fully formed. At a drift-ratio of 1.7%, yielding spread across the gaged bars. In specimen C-02, punching initiated on the north side of the column at a drift-ratio of 2.44% and completed when a drift-ratio of 2.4% was applied on the following, southern drift excursion.

When upgraded with CFRP shear reinforcement, specimens A4-S and B4-S (Figures 7 and 8) had significant increases in ductility and energy dissipation capacities when compared with control specimens. The upgraded test specimens displayed similar behavior to the control specimens until 2.5% inter-story drift, but specimens A4-S and B4-S did not experience a punching shear failure while subjected to combined gravity and lateral loads. Both upgraded specimens sustained substantial reinforcing bar yielding. Flexural cracks on the top slab face of specimens A4-S and B4-S opened wider as drift excursions increased. Increased crack widths augmented pinching in the load-displacement hysteresis loops at larger drift-ratios.

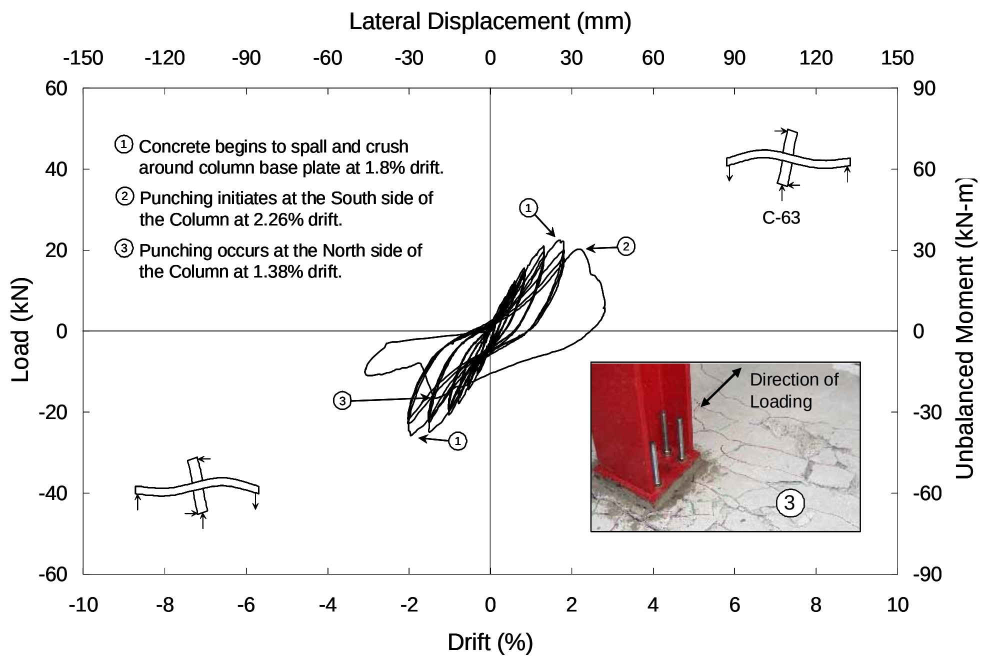

Figure 5. Lateral Load-deformation behavior of specimen C-63

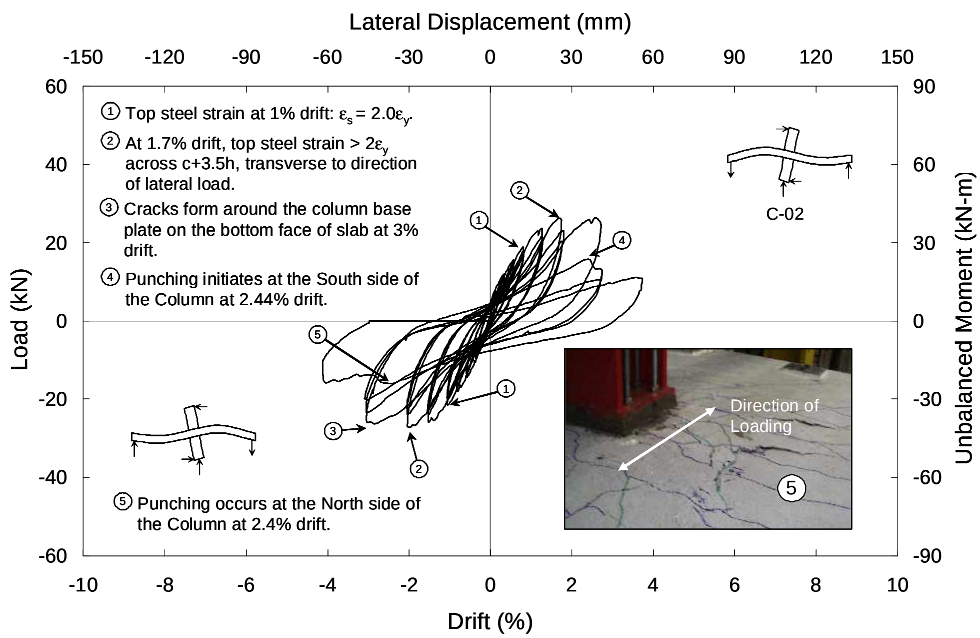

Figure 6. Lateral Load-deformation behavior of specimen C-02

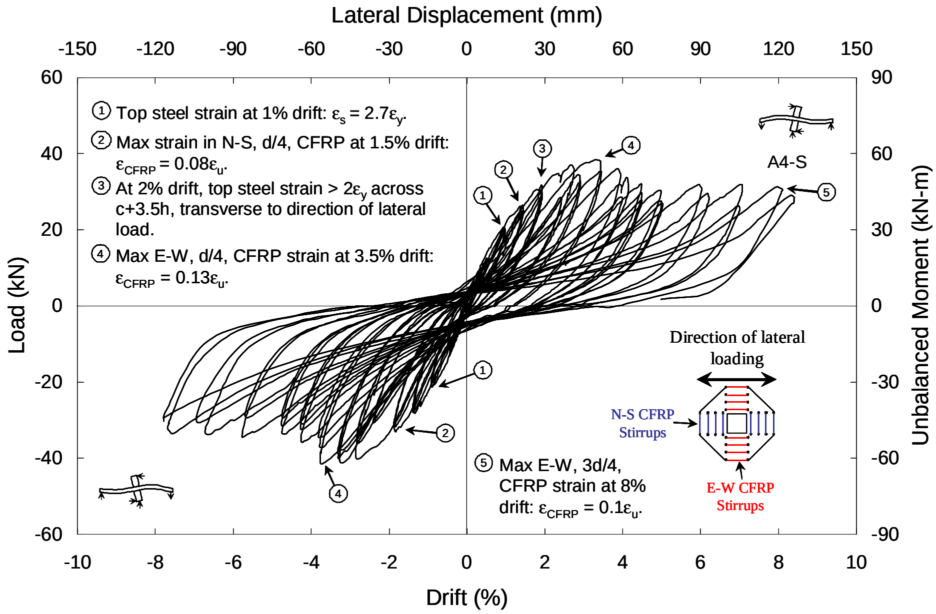

Figure 7. Load-deformation behavior of specimen A4-S

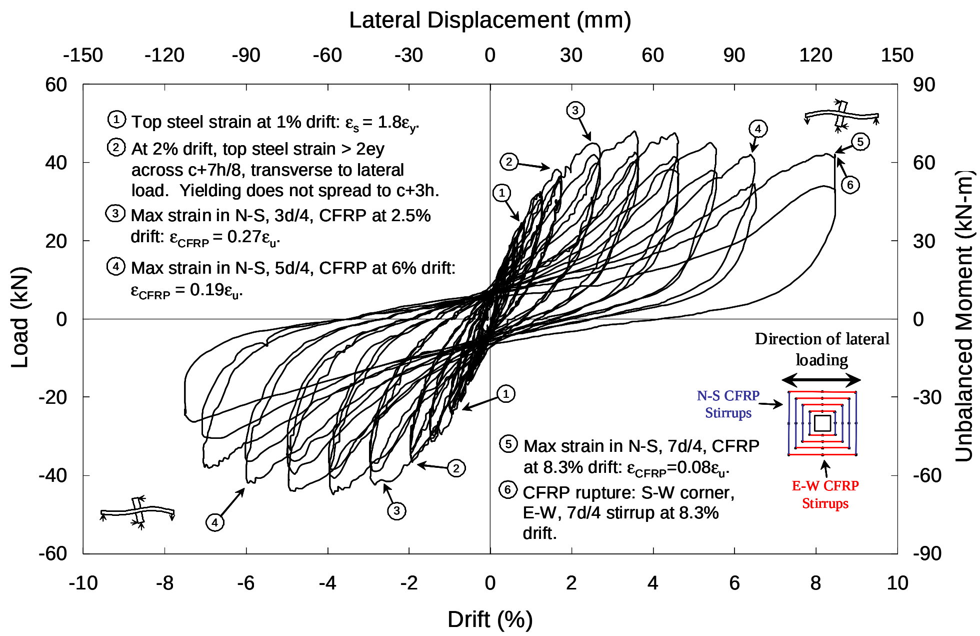

Figure 8. Load-deformation behavior of specimen B4-S

Either of the control specimens did not exhibit ductile behavior. Lateral load-drift backbone curves for each specimen are compared in Figure 9. The poor inelastic behavior displayed by specimens C-63 and C-02 was eliminated in upgraded specimens A4-S and B4-S. After achieving a maximum lateral load of 41.5 kN, specimen A4-S retained 80% of the maximum resisted lateral load up to an inter-story drift of 8.3%. Following the initial strength degradation, the lateral load carrying capacity increased after an applied drift of 7%, due to the onset of strain hardening in the reinforcing steel bars. The maximum lateral load resisted by specimen B4-S was 48 kN. After reaching the peak lateral load peak, specimen B4-S demonstrated a strength decay of 12.5% until CFRP stirrup rupture at the outermost shear reinforcement perimeter occurred at 8.3% inter-story drift. This resulted in a 41% decrease in lateral load resistance on the completion of the applied drift-cycle. The increase in lateral load resistance by the upgraded test specimen was 52% greater than C-02 for test specimen A4-S, and 77% greater for test specimen B4-S. This could be attributed to the horizontal components of the CFRP stirrups bonded on the slab tension surface acting as flexural reinforcement.

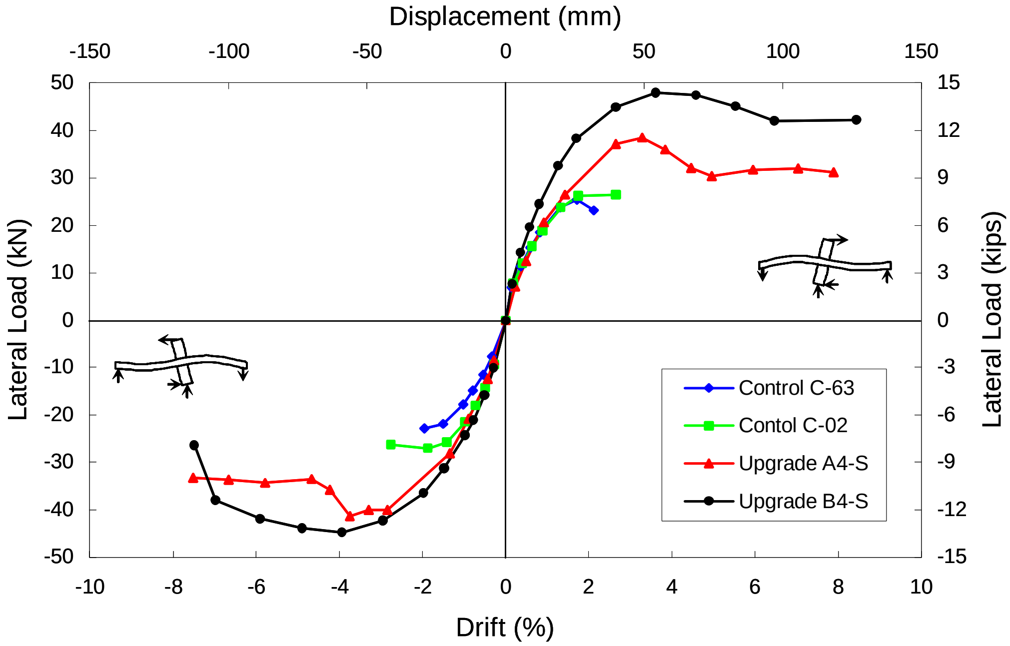

Figure 9 Backbone curves for test specimens

Table 1 presents CFRP strains at different shear reinforcement perimeters for upgraded specimens A4-S and B4-S at different load stages. CFRP strain measurements for these two specimens showed similar characteristics. CFRP stirrups located at the first two perimeters experienced significant strains up to approximately 2.5% drift-cycle. This level of deformation corresponds to punching failure of the control specimen. Beyond a drift level of about 3%, CFRP strains at the first two perimeters decreased and the vertical strains in the shear reinforcement perimeters at 5d/4 and 7d/4 away from the column started to increase. This is an indication that CFRP stirrups at the first two perimeters were activated when the inclined crack crossed these stirrups at a drift ratio of about 2.5%. Beyond this drift level, due to the formation of additional inclined cracks crossing the last two CFRP perimeters, CFRP vertical legs in the first two perimeters unloaded. Simultaneously, CFRPs at the last two perimeters started carrying significant forces. These results show that contribution of CFRP stirrups located at first two and last two perimeters took place at different times and magnitudes as the punching critical zone was shifted away from the connection area. Maximum vertical CFRP strains were 0.0017 and 0.0032 for specimens A4-S and B4-S, respectively. CFRP rupture occurred at the corners of the outermost shear reinforcement in specimen B4-S. This shows that higher strains were experienced at locations of stress concentrations than measured along vertical legs.

Table 1. Comparisons of vertical CFRP strains

Specimen	Measurement Locations*	CFRP Strains (% strain) at Various Drift Ratio (%)								
		0 (Gravity)	1	2	3	4	5	6	7	8
A4-S	1	0.03	0.09	0.09	0.13	0.15	0.12	0.11	0.09	0.17
	2	0.01	0.02	0.03	0.07	0.12	0.11	0.13	0.14	0.15
	3	0.02	0.01	0.04	0.06	0.08	0.07	0.07	0.08	0.08
	4	0.01	0.03	0.06	0.07	0.05	0.04	0.04	0.04	0.04
B4-S	2	0.1	0.22	0.3	0.13	0.13	0.14	0.13	0.12	0.12
	3	0.04	0.1	0.13	0.2	0.19	0.21	0.22	0.2	0.2
	4	0.03	0.04	0.05	0.06	0.07	0.08	0.09	0.09	0.1

*: Locations as given per Figure 2.

EVALUATION OF SEISMIC PERFORMANCE OF TEST SPECIMENS

Definitions

A consistent basis for quantifying specimen behavior is established to evaluate seismic performance of the control and upgraded test specimens. The displacement ductility factor (μ_Δ), cumulative ductility ratio (N_Δ) and work and energy-damage indicators (W) are used to comparatively study the response of the specimens. Figure 10 defines the ductility parameters used to evaluate the post-elastic behavior of the test specimens in the study. All ductility parameters definitions used in this study were defined by Ehsani and Wight [25].

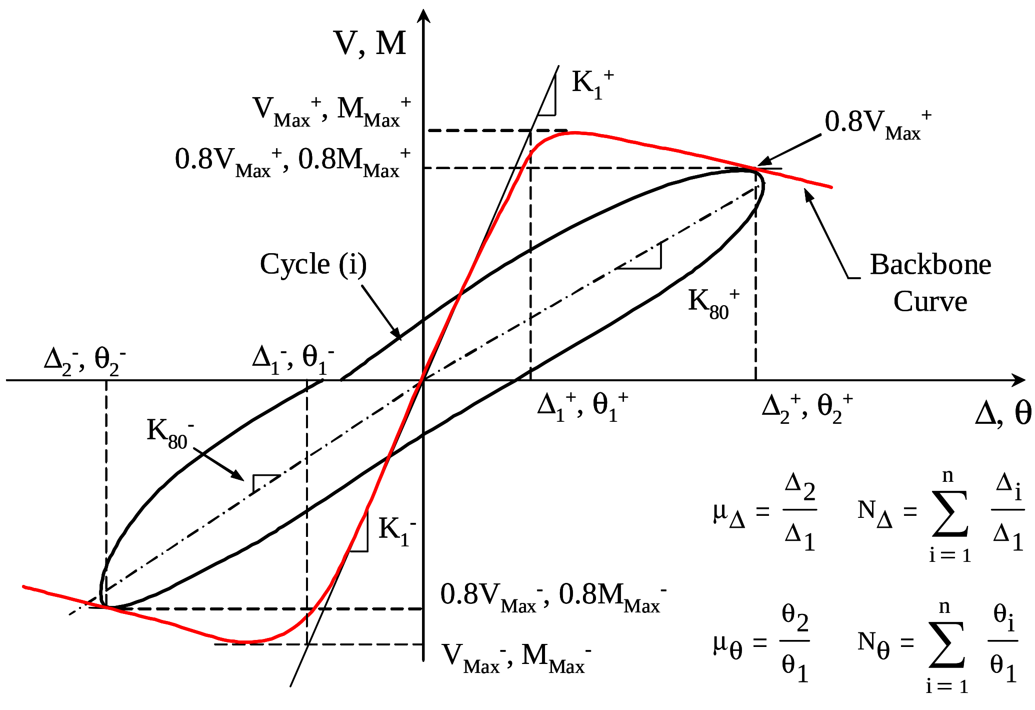

Figure 10 Definition of Ductility Parameters

Displacement ductility factors (μ_Δ) are calculated from the backbone curves shown in Figure 9. Δ_1 is the yield displacement as shown in Figure 10. Δ_2 is the displacement corresponding to a 20% reduction in lateral load and unbalanced moment capacity on the descending branch of the each backbone curve. The ductility factors used in this study are defined as the ratio of Δ_2 to Δ_1 and are presented for both the directions of lateral loading.

The cumulative displacement ductility ratio (N_Δ) is defined in Figure 10. These parameters are also determined using the backbone curves from Figure 9. As can be seen in Figure 10, N_Δ is the cumulative ratios of the peak displacement at the ith drift-cycle (Δ_i) normalized to the yield displacement (Δ_1). Two ductility ratios are presented for lateral load-displacement data. $N_{\Delta 80}$ is the cumulative ductility ratio corresponding to the drift-cycle where a 20% reduction in lateral load occurs on the descending branch of a given backbone curve. The total displacement ductility ratio, $N_{\Delta t}$, is the collective summation of the ductility ratios from the entire test.

In this study, an index is used to quantify the amount of energy dissipated within each specimen's slab-column connection during each drift-cycle: the work-damage indicator, W. The work damage indicator represents the work done on a test specimen by the applied lateral load. Equation (1) defines the work-damage indicator.

$$W = \frac{1}{V_{Max} \cdot \Delta_1} \cdot \sum_{i=1}^{n} w_i \cdot \left(\frac{K_i}{K_1} \right) \cdot \left(\frac{\Delta_i}{\Delta_1} \right)^2 \qquad \textbf{\textit{(1)}}$$

where V_{Max} is the average of V_{Max}^{+} and V_{Max}^{-}; w_i is the energy dissipated in the ith drift-cycle (calculated from the area of the ith load-displacement loop) Δ_1 is the average of Δ_1^{+} and Δ_1^{-} ; Δ_i is the average of Δ_i^{+} and Δ_i^{-}; K_1 is the average of K_1^{+} and K_1^{-}; and K_i is the average of K_i^{+} and K_i^{-} (Figure 10). Work-damage is calculated for the cumulative drift-cycles until a 20% loss of the maximum lateral load (W_{80}) and for the total number of drift-cycles in a test (W_t).

Lateral Load-Displacement Ductility Parameters

The post-elastic, lateral load deformation behavior of the tested slab-column connections significantly improved when upgraded using CFRP stirrups. This is evidenced by the lateral load-deformation ductility parameters listed in Table 3. The lateral displacement ductility factor of both of the upgraded specimens was two times that of control specimen C-02, when "pushed" in the south direction. When the specimen was "pulled" in the north direction, the ductility factor of specimen B4-S dropped to 1.75 times that of C-02 due to CFRP rupture. However, these ductility measurements indicated that both the upgraded specimens had stable descending branches and that they sustained significant inelastic deformations without losing strength.

A similar pattern was found in the cumulative ductility ratio parameters. Specimens A4-S and B4-S both had ductility ratios, $N_{\Delta 80}$ and $N_{\Delta t}$, more than two times greater than that of specimen C-02. A4-S had equivalent $N_{\Delta 80}$ and $N_{\Delta t}$ ratios because the lateral load did not drop below 80% of maximum value over the duration of the test. The ductility ratios $N_{\Delta 80}$ to $N_{\Delta t}$ of specimen A4-S were also 30% and 18% greater than those of specimen B4-S.

The work-damage indicators, W_{80} to W_t, more than tripled for test specimens A4-S and B4-S over control specimen C-02. This indicates the energy dissipation characteristics of test specimens A4-S and B4-S were much greater than the control specimens. The addition of CFRP shear stirrups increased the punching shear strength of specimens A4-S and B4-S. This allowed the upgraded specimens to sustain significant inelastic lateral deformations. Larger load-deformation hysteresis loops were therefore generated because more energy was absorbed from the lateral loads acting upon the upgrade specimens. Specimens A4-S and B4-S dissipated almost the same amount of total energy during the lateral load tests. However, the energy dissipation characteristics of specimen A4-S are somewhat better because connection upgrade A4-S maintained 80% of the lateral load capacity over the duration of the test.

Stiffness Degradation

The stiffness degradations of the test specimens are presented in Figure 11. The initial lateral stiffness of test specimen B4-S was found to be 3% greater than control specimen C-02. Therefore, the additional CFRP stirrups had insignificant affects on the initial lateral stiffness of the test specimens in this study.

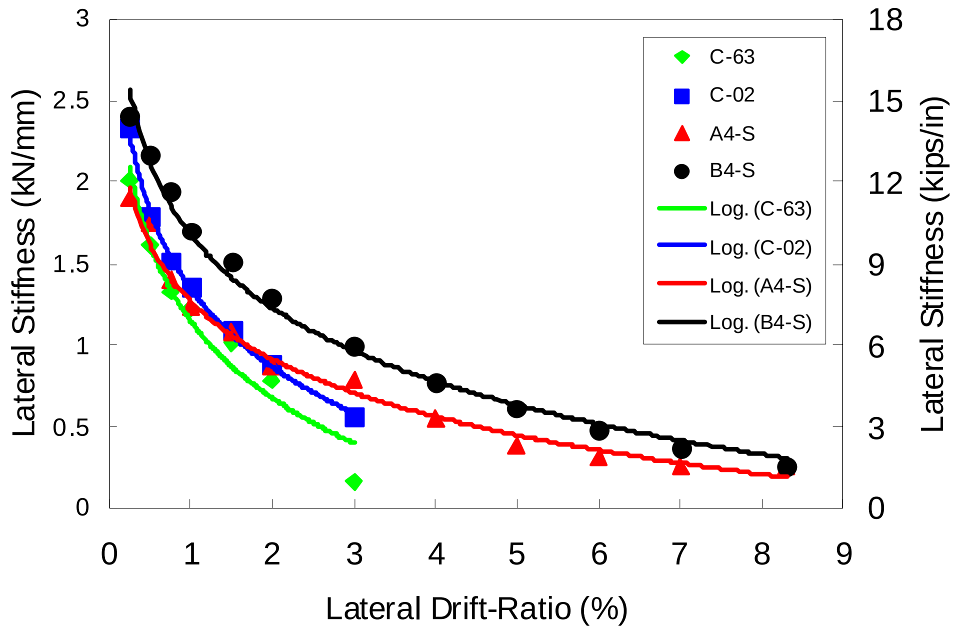

Figure 11 Peak lateral stiffness versus applied drift-ratio

With gradually increased inelastic deformation cycles, the upgraded test specimens exhibited greater lateral stiffness values when compared to the control specimens. The lateral stiffness of control specimen C-02 and C-63 rapidly degraded at each applied drift-cycle until punching shear failures occurred. Despite having the lowest initial stiffness, the lateral stiffness decay of specimen A4-S decreased compared with each control specimen at an applied drift-ratio of 1.5%. Specimen A4-S displayed stable hysteretic response with gradual stiffness degradation at large inelastic deformation cycles. The stiffness decay of specimen B4-S paralleled specimen A4-S, but specimen B4-S had somewhat greater stiffness through the test.

The lateral stiffness degradation of each specimen was correlated to the amount of damage incurred at the connection region. Lateral stiffness of specimens A4-S and B4-S did not degrade as rapidly as the control specimens because the CFRP stirrups prevented the formation of large cracks and associated damage in the joint region. Cracking occurred in the connection region of the upgraded specimens, however, cracks propagated through the holes in the slabs along the face of the column base plate, transverse to the direction of loading. Cracks spread throughout the connection region, which ultimately resulted in punching shear failure. Of the upgraded specimens, A4-S showed the least amount of damage in the connection region.

SUMMARY AND CONCLUSIONS

The main objective of the study was to investigate the response of interior reinforced concrete flat-plate connections upgraded with CFRP stirrups to simulated seismic loads. Test specimens in the study included flat-plate slabs designed according to ACI 318-63 and ACI 318-02 requirements and two flat-plate connections upgraded with additional CFRP stirrups positioned radially around the slab-column interface. Based on the results of the study, the following conclusions can be made:

1) Applying CFRP stirrups in radial patterns around the slab-column connections of flat-plate structures is a structurally feasible method of upgrading the connection for seismic loading conditions. When CFRP shear reinforcement was provided at the slab-column connection, punching shear failure was prevented and the failure mode changed to flexure. This enabled the upgraded specimens to display ductile behavior, whereas the control specimens exhibited punching shear failures.

2) Upgrading the slab-column connections using CFRP stirrups significantly increased the drift capacity of the connection. Results from testing show that specimens A4-S and B4-S both had increases in lateral drift capacity of about three times that of control specimen C-02. Specimen C-02 exhibited a punching shear failure at a lateral drift of 2.4%, whereas specimens A4-S and B4-S both attained lateral drift ratios of 8.3%. It should be noted that these drift ratios achieved by specimens A4-S and B4-S are unrealistic when they are compared with code limits and reasonable drift levels in real flat-plate structures. However, if this method of upgrading slab-column connections can result in large inter-story drift capacities while subjected to large gravity loads, the performance of these upgraded connections should be adequate in less demanding conditions.

3) The connection rotation capacity of the upgraded test specimens was also improved with the addition of CFRP stirrups. An increase in rotational capacity of over 200% was shown in test specimen B4-S. Specimen A4-S had measured increases in rotational capacity of 130%, which were limited by the saturation of readings from rotation instruments. It is believed that if rotation instruments were able to record data through the duration of the test, the increase in connection rotation capacity of specimen A4-S would be similar to B4-S.

4) Strengthening the region adjacent to the column faces shifted the critical perimeter of the slab-connections of the upgraded specimens, which prevented punching shear failure and allowed these specimens to deform inelastically, in a stable manner. This was confirmed with the measured CFRP strains and observed CFRP contributions in carrying excessive shear forces.

5) The upgraded test specimens dissipated considerably more amounts of energy than the control specimens. The energy-damage indicator showed the greatest increase, being 8-10 times greater for the upgraded test specimens than control specimen C-02. The work-damage indicator of the upgraded test specimens was 4-times that of specimen C-02. Both cumulative displacement and rotation ductility ratios increased 3-4 times that of specimen C-02 and the displacement and rotation ductility factors were 2-3 times greater than the control specimen.

6) Test results show that flat-plate slab-column connections upgraded with CFRP stirrups did not experience a radical change in the lateral stiffness. A maximum stiffness increase was measured to be 3%. Stiffness degradation did not occur as rapidly in the upgraded test specimens, in comparison to the control specimens. As the lateral displacement excursions increased, the stiffness of the upgraded specimens did not degrade rapidly because the CFRP stirrups helped to mitigate damage within the connection region.

REFERENCES

1- Hawkins, N. W., "Shear Strength of Slabs with Shear Reinforcement," ACI Publication SP-42, Shear in Reinforced Concrete, 1974, 785-816.

2- Seible F., Ghali, A., Dilger, W. H., "Preassembled Shear Reinforcing Units for Flat Plates," ACI Journal Proc., 77(1), 1980, 28-35.

3- Hanson N. W., and Hanson, J. M., "Shear and Moment Transfer between Concrete Slabs and Columns," Journal, PCA Res. and Devel. Labs., 10(1), 1968, 1-16.

4- Islam S., and Park. R., "Tests on Slab-column Connections with Shear and Unbalanced Flexure," J. Struct. Div. 102(3), 1976, 549-568.

5- Ghali, A., Elmasri, M.Z., and Dilger, W., "Punching of Flat-plates under Static and Dynamic Horizontal Forces," ACI J., 73(10), 1976, 566-572.

6- Morrison, D. G., Hirasaqa, L. and Sozen, M.A., "Lateral-Load Tests of R/C Slab-Column Connections," ASCE Journal of Structural Division, V.109, No.11, 1983, 2698-2714.

7- Zee H. L., and Moehle J. P., "Behavior of Interior and Exterior Flat Plate Connections Subjected to Inelastic Load Reversals," Report UCB/SEEM-84/07, Dept. of Civil Eng., University of California, Berkeley, California, 1984.

8- Pan., A., Meohle., J.P., "Reinforced Concrete Flat Plates under Lateral Loading: An Experimental Study Including Biaxial Effects," Report No. UCB/EERC88/16. College of Engineering, University of California at Berkeley, 1998.

9- Dilger, W., and Cao, H., "Behavior of Slab-column Connections under Reversed Cyclic Loading," Proc., 2nd Int. Conf. of High-Rise Buildings, China, 1999.

10- Robertson, I. N., and Durrani., A. J., "Seismic Response of Connections in Indeterminate Flat-slab Assemblages," Struct. Res. at Rice, Rep. 41, Dept. of Civil eng., Rice University, Houston, Texas, 1990.

11- Durrani, A. J., and Du. Y., "Seismic Resistance of Slab-column Connections in Existing Non-ductile Flat Plate Buildings," Tech Report NCEER-92-0010, State University of New York, Buffalo, N.Y, 1992.

12- Hwang S. J. and Moehle J. P., "An Experimental Study of Flat Plate Structures under Vertical and Lateral Loads," Report UCB/SEEM-90/11, Dept. of Civil Eng., University of California, Berkeley, Calif, 1993.

13- Luo Yh, Durrani A, Conte J, "Seismic Reliability Assessment of Existing R/C Flat-Slab Buildings," J. of Struct. Eng., ASCE, 121(10), 1995, 1522-1530.

14- Hueste M.B.D., Wight, J.K., "Nonlinear Punching Shear Failure Model for Interior Slab-column Connections," ASCE, Journal of Structural Eng., 125(9), 1999, 997-1008

15- Moehle, J.P., Kreger, M.E., Leon, R., "Background to Recommendations for Design of Reinforced Concrete Slab-Column Connections," ACI Structural Journal. Vol. 85, No. 6, 1988, 636-644.

16- Martinez-Cruzoda, J.A., Qaisrani, A.N., Moehle, J.P., "Post-Tensioned Flat Plate Slab-Column Connections Subjected to Earthquake Loading," Proceedings, Fifth U.S. National Conference on Earthquake Engineering, Vol. 2, Chicago, Illinois, 1994, 139-148.

17- Farhey, D.N., Adin, M.A. and Yankelevsy, D.Z., "Repaired RC Flat Slab-Column Connection Subassemblages under Lateral Loading," J. of Struct. Eng., ASCE, 121(11), 1995, 1710-1720.

18- Ebead, U. and Marzouk, H., “Strengthening of Two-Way Slabs Subjected to Moment and Cyclic Loading,” Structural Journal, ACI, 99(4), 2002, 435-444.

19- El-Salakawy, E.F., Polak, M.A. and Soudki, K.A., “New Shear Strengthening Technique for Concrete Slab-Column Connections,” Struct. J., ACI, 100(3), 2003, 297-304.

20- Hassanzadeh, G. and Sundqvist, H., “Strengthening of Bridge Slabs on Columns,” Nordic Concrete Research 1/1998, No. 21, 1998.

21- Stark, A., “Seismic Upgrade of Flat-Plate Slab-Column Connections using Carbon Fiber Reinforced Polymer Stirrups,” Master’s Thesis, Department of Civil Engineering, The University of Texas at Austin, August 2003.

22- ACI Committee 318, “Building Code Requirements for Structural Concrete (ACI 318-02),” American Concrete Institute, Farmington Hills, Michigan, 2002.

23- Binici, B., “Punching Shear Strengthening of Reinforced Concrete Slabs Using fiber Reinforced Polymers,” Dissertation submitted to The University of Texas at Austin in partial fulfillment of the requirements of Doctor of Philosophy, 2003, 279 pp.

24- T1.1-01/T1.1R-01: Acceptance Criteria for Moment Frames Based on Structural Testing, American Concrete Society, 2001, 10 pp.

25- Ehsani, M.R. and J.K. Wight, “Confinement Steel Requirements for Connections in Ductile Frames.” ASCE Journal of Structural Engineering, Vol. 116, No. 3, Mar. 1990, pp. 751-767.